Experiments with compressively sampled images and a new debluring-denoising algorithm

Sina Jafarpour
Computer Science
Princeton University
sina@cs.princeton.edu

Ali Pezeshki
Applied Mathematics
Princeton University
pezeshki@math.princeton.edu

Robert Calderbank
Electrical Engineering
Princeton University
calderbk@math.princeton.edu

***Abstract*—In this paper we will examine the effect of different parameters in the quality of real compressively sampled images in the compressed sensing framework. We will select a variety of different real images of different types and test the quality of the recovered images, the recovery time, and required resources when different measurement methods with different parameters are used or when different recovering methods are applied. Then we will propose an algorithm to reduce the noise in the recovered images and sharpen them simultaneously. The algorithm exploits a well-known bilateral filtering in order to increase the confidence in margins and edges, and then uses an adaptive unsharp mask method to sharpen the images. The adaptive unsharp mask method extends the ordinary unsharp mask method and uses machine learning square loss minimization and regression in order to learn the optimal unsharping parameters. We will argue why both bilateral filtering and unsharp mask methods should be used in the algorithm simultaneously. Finally, we will show the results of applying the algorithm on real images that are recovered using the compressed sensing method and we will interpret the experimental results.**

I. Introduction

Recently, a novel way of sampling signals has been proposed capable of bypassing the Nyquist's sampling limits for a variety of signals [9], [10], [11]. One class of signals for which the compressed sensing approach works is the images, which are two dimensional piecewise-smooth signals, with only a few large coefficients in the wavelet domain. Furthermore a recent brand of cameras called the single pixel cameras [16] has been produced that can perform the compressed sensing measurements very efficiently. However, it is very important to choose the parameters influencing the measurement and recovery wisely. Good parameters will lead to high quality images that can be recovered efficiently and need cheap resources such as memories and processors; on the other hand, if the parameters are set inappropriately, the result may be even worse than the traditional sampling-compressing method. Most of the experimental results in compressed sensing are done on artificially made data sets or on a very specific set of images and not on different real images of different types. Furthermore, most of the experiments were only concerning one particular aspect of the recovering problem alone. Among the papers with a more general and practical experimental approach are [7] [9]. Following their work in this paper, several compressed sensing experiments has been done and the effect of different approaches and parameters on the quality and efficiency of the recovered images has been investigated.

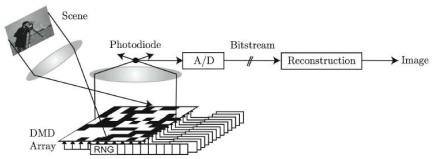

Fig. 1. Single Pixel Camera from [12]

The other benefit of using several real images of different kinds will be the ability to train the parameters of an adaptive unsharp mask method in order to increase the quality of the recovered images. Generally, the recovered images are noisy, also the recovered image will be too smooth. In this paper we will propose an algorithm that eliminates the noise and adaptively sharpens the image simultaneously. The algorithm exploits both a bilateral filtering method [18], [17] that enhances the marginal confidence images and one adaptive generalization of the unsharp mask method [20] that uses the square loss minimization and regression which are machine learning techniques [21] in order to eliminate the noise and sharpen the image so that the image does not lose its natural look. We will argue why both parts are needed in the quality enhancement algorithm and why none of them can enhance the quality of the recovered image very much solely. We will train our algorithm with various images which are the results of compressed sensing recovery method and then we will use the optimal parameters in order to increase the quality of a recovered test image.

The structure of the paper will be as follow: In the next subsections we will define the compressed sensing precisely. Next, we will show why compressed sensing is very appropriate in image sampling and compression. Experimental results about choosing good parameters in compressed sensing go next. Then will describe the bilateral filtering and adaptive unsharp mask methods. Finally, we will use these two methods to propose our image quality improvement algorithm; furthermore, we will show the result of applying the algorithm on real images which directly recovered using the compressed sensing methods.

978-0-7695-3454-1/08 $25.00 © 2008 IEEE
DOI 10.1109/ISM.2008.119

II. WHAT IS COMPRESSED SENSING?

The goal of *compressive sampling* or *compressed sensing* [9], [10], [11], is to replace the common pointwise signal sampling methods with a new different sampling approach in order to increase the sampling rate to more than what the Nyquist's theorem [12] says and still be able to recover the signal from the samples. From the classic signal processing theorems it is well known that the Nyquist's theorem states that generally this task is impossible. However, if the signals are sparse, one can come over the Nyquist's limitations using a different sampling framework [13], [14]. In order to make it simper, we will show the sampling approach by a game between two players Alice and Bob. For now, we assume that the signal is a discrete signal with n components. So the signal x can be seen as an arbitrary vector in R^n. Before describing the game we need to define the k-sparseness and almost-k-sparseness:

Definition 1 (k-sparseness): A signal $x \in R^n$ is k-sparse iff there exists a basis in which the signal has at most k non-zero elements.

Definition 2 (almost-k-sparseness): A signal $x \in R^n$ is almost-k-sparse iff there exists a basis in which except at most k elements of x, all the other elements have norm very close to zero.

Now the compressed sensing problem, the game between Alice and Bob, is as follow: Suppose Bob has an almost k-sparse signal x. Alice's task is to ask as few questions of a certain kind, known as samples from x, as possible from Bob and then she should come up with a signal $\hat{x}$ as close to x as possible. In compressed sensing these samplings are done by linear measurements instead of pointwise sampling. Meaning that at each round t Alice gives a vector $\langle A_t|$ and then receives the inner product $\langle A_i|x\rangle$ as the measurement result. So her task is to find a $m * n$ matrix A such that m , the number of measurements, becomes as small as possible and x can be approximately recovered efficiently from $y = Ax$. It is obvious that generally it is impossible, but the sparsity of x gives a chance that by choosing a proper measurement matrix A one may be able to recover x from y.

The framework above suggests a way of compressing the image during the process of sampling. In the usual approaches first a signal is totally sampled using n pointwise samplings, then it is transformed to the basis in which it is sparse, then it is compressed by writing down the value and position of non-zero elements (and typically ignoring the small value elements if the signal is almost-k-sparse). So the compressed image will have size $O(k \log n)$. However, this process needs additional intermediate time and space resources. In contrast, in compressed sensing mode, as we will show later one can find good measurement matrices such that $m = O(k \log n)$ samplings are enough in order to be able to recover the signal x from the measurements y efficiently. So by using compressed sensing instead of usual sampling-compression method one can bypass the traditional Nyquist's sampling rate and reduce the unnecessary intermediate steps in compressing a signal[1].

Before introducing good measurement and recovery methods, we will define a few terminologies which we will use more often later:

Definition 3: Suppose $A_{m\times n}$ is used as the measurement matrix in compressed sensing, then m is called the sketch size, A is called the sketch matrix and the ration $\frac{m}{n}$ is called the compression rate.

In this paper, we will focus on the geometric approach in recovering sparse signals. This approach uses the common convex programming techniques [9], [10] and is based on the following theorem[2].

Theorem 1 ($l1$-minimization recovering algorithm): Suppose x is an k-sparse signal in R^n and $A_{m\times n}$ is a matrix satisfying some **Null-Space-Property** [13]. Then given $y = Ax$ the following linear optimization problem will always recover x:

$$[l_1\text{minimization}]\ \textbf{min}\ |x'|_1\ \textbf{such that}\ Ax' = y.$$

Also, if x is almost-k-sparse, the program 1 will recover a k-sparse signal $\hat{x}$ such that for any other k-sparse signal x' we have :

$$|x - \hat{x}|_2 \leq C|x - x'|_2$$

for some constant C.

Theorem 1 gives a very general recovering algorithm in compressed sensing. However, for a particular subclass of piecewise smooth signals there is a slightly different model which yields better results. The two dimensional piecewise smooth signals are almost sparse in the wavelet domain, so instead of using $l1$-minimization in the wavelet domain a sparse approximation of the image gradient is recovered using a quadratic programming method called **min TV**. This method is described in more detail in [9], [7], [10] and we only explain it here briefly.

Definition 4 (Total variance norm of a signal): Suppose x is a two dimensional piecewise smooth signal, the ***total variance (TV)*** norm of the signal is defined as :

$$|x|_{TV} = \sum_{i,j} \sqrt{(x_{i+1,j} - x_{i,j})^2 + (x_{i,j+1} - x_{i,j})^2}$$

Then the following theorem states that for this class of signals one can use the *TV norm* minimization program instead of the general Manhattan norm minimization:

Theorem 2 (min TV recovering algorithm): Suppose x is an almost k-sparse signal in R^n where n is a square of an integer, and $A_{m\times n}$ is a matrix satisfying some **Null-Space-Property** [13]. Then given $y = Ax$, the following convex optimization problem:

$$[\text{min TV}]\ \textbf{min}\ |x'|_{TV}\ \textbf{such that}\ Ax' = y.$$

[1]please note that if n becomes too large, the intermediate step in the traditional method may take a very long $O(poly(n))$ time

[2]We will not go through the null space property, we will just mention it here and later show some matrices satisfying this property

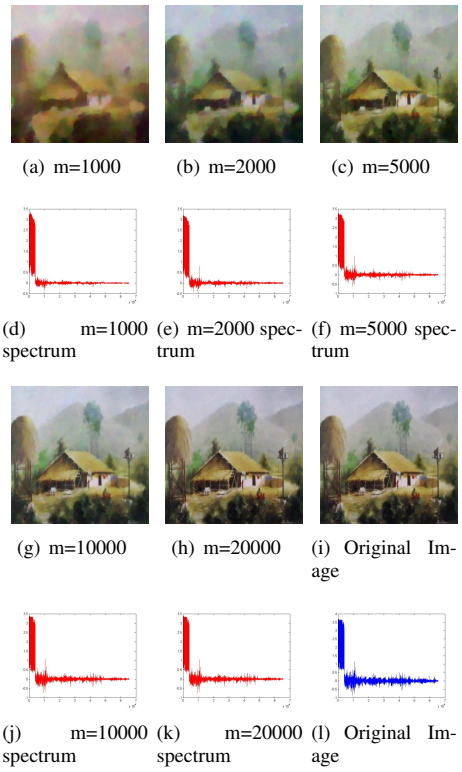

(a) m=1000 (b) m=2000 (c) m=5000

(d) m=1000 spectrum (e) m=2000 spectrum (f) m=5000 spectrum

(g) m=10000 (h) m=20000 (i) Original Image

(j) m=10000 spectrum (k) m=20000 spectrum (l) Original Image

Fig. 2. Recovered images from a 256×256 Scene photo using random Fourier Ensemble and their wavelet spectrum.

will recover a piecewise smooth signal $\hat{x}$ [3] that approximates the original signal with a high precision.

So far, we showed that the Null-Space-Property (NSP) of the measurement matrix allows the recovering of the sparse signals to be done using convex programming methods. In order to show matrices that satisfy this property we need a set of definitions and lemmas:

Definition 5 (Real-valued Random Fourier Ensemble): Suppose $\Omega_{m\times m}$ is the discrete Fourier transform matrix [10], [7]. The Real-valued Random Fourier Matrix $A_{m\times n}$ is a matrix which is obtained by randomly permuting the columns of Ω, selecting a random subset of size $\frac{n}{2}$ of the rows , and separating the real and complex values of each element into two real values. [9]

The following norm preservation property for random Fourier ensembles has its origin from the dimensionality reduction techniques and is a direct consequence of the well-known *Johnson-Lindenstrauss* lemma in machine learning [15].

Definition 6 (Restricted Isometry Property for l_2 Norm): Matrix $A_{m\times n}$ satisfies the Restricted Isometry Property (RIP-2) for Euclidean Norm with RIP-value equal to l, iff $\exists \epsilon > 0$ such that with very high probability $\forall$ l-sparse signal x the following condition holds:

$$(1-\epsilon)|x|_2 \leq |Ax|_2 \leq (1+\epsilon)|x|_2$$

[3]with sparse gradient

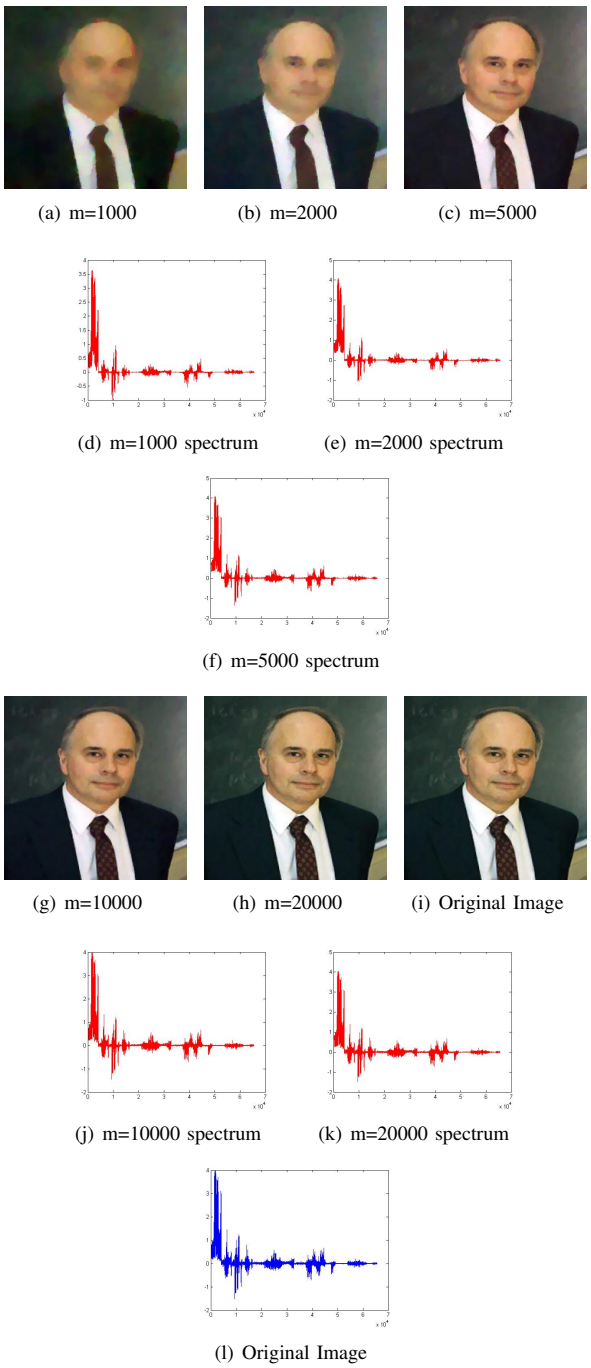

(a) m=1000 (b) m=2000 (c) m=5000

(d) m=1000 spectrum (e) m=2000 spectrum

(f) m=5000 spectrum

(g) m=10000 (h) m=20000 (i) Original Image

(j) m=10000 spectrum (k) m=20000 spectrum

(l) Original Image

Fig. 3. Recovered images from a 256*256 Portrait photo using random Fourier Ensemble and their wavelet spectrum.

In other words, the RIP-2 property states that the projection preserves the Euclidean norm of any l-sparse vector [12].

Lemma 1: Let $m = \theta(k \log n)$ and let $A_{m \times n}$ be a real-valued random Fourier ensemble[4]. Then A satisfies the norm-2 RIP property with RIP-value $3k$.

Lemma 2: If matrix A satisfies the norm-2 RIP property with RIP-value $3k$ then A satisfies the Null Space Property.

Corollary 1: If $m = \theta(k \log n)$ then the real-valued Fourier ensemble $A_{m \times n}$ satisfies the Null Space Property.

Remark: Although other random projection-based matrices such as Gaussian matrices also satisfy the Null Space Condition, we will use the real-values random Fourier scramble. The reason is that we can use this ensemble with $O(n)$ space usage and $O(n \log n)$ multiplication time, making this matrix feasible for experiments with large signals [7].

Definition 7 (Expander Graphs, informally [2]): An expander graph E is a d regular graph with v vertices, such that:

1) E is sparse (ideally d is much smaller than v).
2) E is *" well connected"*.

Definition 8 ($(k, 1-\epsilon)$ lossless unbalanced expander graph): A $(l, 1-\epsilon)$-*unbalanced bipartite expander graph* is a bipartite graph $E = (A, B), |A| = n, |B| = m$, where A is the set of variable nodes and B is the set of parity nodes, with regular left degree d such that for any $X \subset A$, if $|X| \leq l$ then the set of neighbors $N(X)$ of X has size $N(X) > (1-\epsilon)d|X|$.

Lemma 3: for any $\frac{n}{2} \geq l \geq 1$, $\epsilon > 0$ there exists a $(l, 1-\epsilon)$ expander with left degree:

$$d = O\left(\frac{\log(\frac{n}{l})}{\epsilon}\right)$$

and right set size:

$$m = O\left(\frac{l \log(\frac{n}{l})}{\epsilon^2}\right).$$

Furthermore, any left-regular random graph with very high probability satisfies the expansion property [3], and also it is possible to explicitly construct the adjacency matrix of a $(k, 1-\epsilon)$ expander graphs with $m = O(poly(\log n))$ [8].

Definition 9 (Restricted Isometry Property for l_1 Norms [7]): Let $A_{m \times n}$ be given. We say that A satisfies the Restricted Isometry Property for Manhattan Norms (RIP-1) with RIP-value equal to l, if for any l-sparse vector $x \in \mathcal{R}^n$ we have:

$$(1-2\epsilon)\ d\ ||x||_1 \leq ||Ax||_1 \leq d\ ||x||_1$$

In other words, the RIP-1 property states that the projection preserves the Manhattan norm of any l-sparse vectors.

Lemma 4: Let $A_{m \times n}$ be the adjacency matrix of a $(3k, 1-\epsilon)$ expander graph E, then A satisfies the Restricted Isometry Property for Manhattan norms with RIP-value equal to $3k$.

Lemma 5: If matrix A satisfies the RIP-1 property with RIP-value equal to $3k$ then A satisfies the Null Space Property.

[4]Other random projection matrices such as Random Gaussian Ensemble and Random Bernoulli matrices are also appropriate.

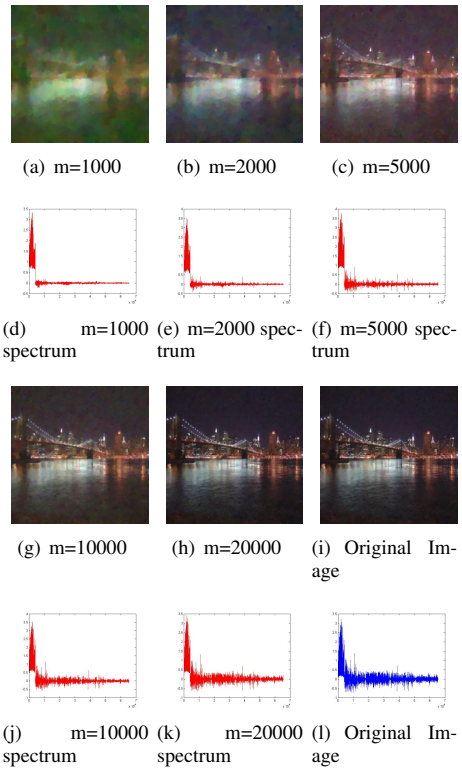

(a) m=1000 (b) m=2000 (c) m=5000

(d) m=1000 spectrum (e) m=2000 spectrum (f) m=5000 spectrum

(g) m=10000 (h) m=20000 (i) Original Image

(j) m=10000 spectrum (k) m=20000 spectrum (l) Original Image

Fig. 4. Recovered images from a 256*256 Night Picture using random Fourier Ensemble and their wavelet spectrum.

Corollary 2: With very high probability the adjacency matrix of any $(n, O(k \log n)$ bipartite, left regular random graph with left degree $d = O(\log n)$ satisfies the Null Space Property. Also explicit sparse matrices satisfying the Null Space Property exists [7].

III. Efficient Compressed Sampling of Images and Recovering

One direct application of compressed sensing is in image compression. Recently a new generation of cameras called *single pixel cameras* [16] have been designed that are capable of performing compressed sensing measurements very efficiently [12]. These brand of cameras let us overcome the Nyquist's limits and eliminate the intermediate traditional compression method. Furthermore, these cameras work more precise and are inexpensive for infrared wavelength. So using these brand of cameras instead of the original cameras will have superior benefits. Moreover, the images are sparse in the wavelet domain, so theoretically the general $l1$-minimization recovering works for them. Also the images are two-dimensional piecewise-smooth signals so the min TV recovering algorithm also finds a very good approximation of these signals.

In the next section we will examine many different real images from different classes [5], and try to find good re-

[5]also these images will be used as the training set for learning the parameters in the enhancing the quality of the recovered images in the next sections

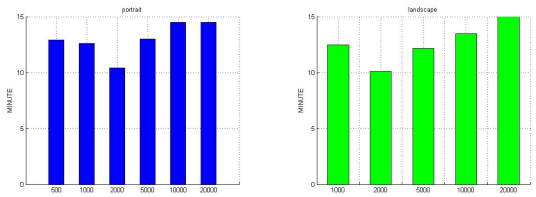

(a) Portrait (b) Scene

(c) Night (d) Painting

Fig. 5. Recovery time of the different images with various number of measurements

covering parameters and compare the different measurement and recovery methods. In particular, we will compare the measurement and recovery techniques mentioned above from different perspectives such as time, memory, etc; to find positions in which using each method has superior advantages over the others. We will later use the original and recovered images from different classes as the training and test sets in order to learn the parameters to enhance the quality of the recovered images even more.

IV. Recovered Images

A. Choosing appropriate compressing rate

It is desirable to find the minimum compression rate such that if a measurement with that rate is performed, it will still be possible to recover an image with a reasonable quality using the recovering algorithm. In order to find the optimal compression rate several 256*256 real photos and paintings where measured with real-valued Fourier ensembles. This is the simulation of the single pixel camera introduced before. Usual cameras support different types of images such as portraits, landscapes, nights, etc, so representative images from all of these types were chosen and the measurement was done on all of them. Then the min TV method which is more restricted to image recovering used to recover the images. The recovered images, plus their wavelet spectrum and signal energy distribution is shown in figure 2 for a scene image, figure 3 for a portrait image, and figure 4 for a picture taken at night for different number of measurements ranging from $m = 1000$ to $m = 20000$.

Also figure 5 shows the recovering time for different images with different number of measurements. It turns out that $m = 5000$ is enough in order to be able to recover an image with acceptable quality. Also the recovering time for $m = 5000$ is efficient[6]. So it turns out that in general about $\frac{m}{n} = \frac{5000}{65536} <$

[6]although there is no essential difference between the recovering times

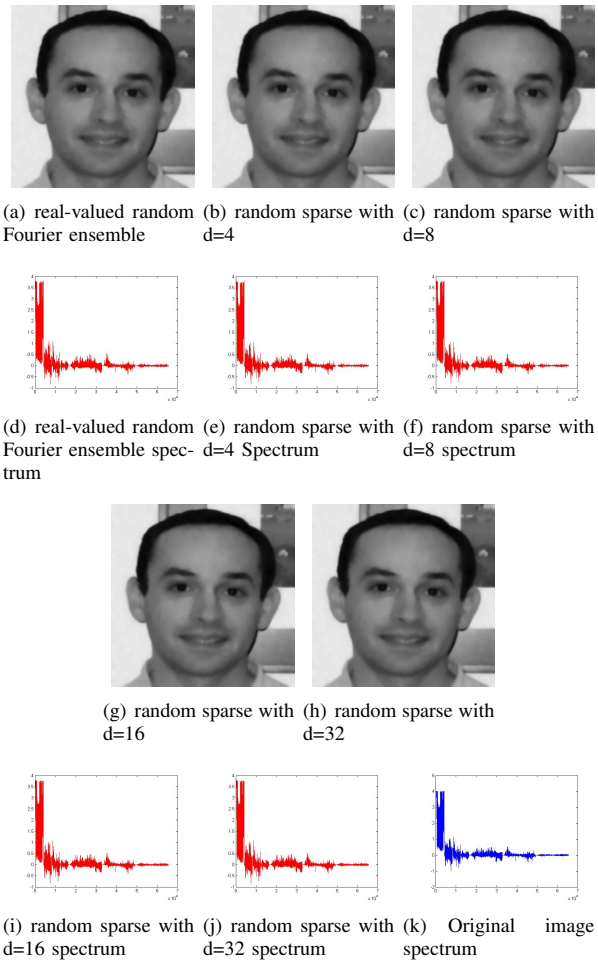

(a) real-valued random Fourier ensemble (b) random sparse with d=4 (c) random sparse with d=8

(d) real-valued random Fourier ensemble spectrum (e) random sparse with d=4 Spectrum (f) random sparse with d=8 spectrum

(g) random sparse with d=16 (h) random sparse with d=32

(i) random sparse with d=16 spectrum (j) random sparse with d=32 spectrum (k) Original image spectrum

Fig. 6. Results of compressed sensing with $m = 8000$ measurements using different measurement matrices, and the wavelet-domain spectrums

10% rate is enough in order to be able to recover an image with reasonable quality. However, if more detail is needed the compression rate has to be increased but about 25% is enough in order to be able to recover almost all detail recognizable by human eye. In the next section we will propose an algorithm to improve the quality of the recovered image.

B. Choosing the recovery method

As we mentioned earlier there are two major geometric image recovering methods : l1-minimization and min-TV. Figure 8 shows an image recovered by these two methods. As this figure and other results for other images and other sketch sizes suggest, the images recovered by the min-TV have much higher quality. This is not something surprising since min TV is a way restricted to images while l1-minimization is a general approach. In contrast, the l1-minimization is about 4 times faster than the min TV method. Hence generally min TV may be the superior image recovering methods. However in special cases that fast recovering is more important than the quality of the recovered images, such as many applications in the

infrared cameras and also in expert systems where only the overall structure of the image is important, l1-minimization may be more appropriate.

C. Choosing the measurement matrix

As we mentioned earlier there are two class of sketch matrices that are appropriate for compressed sensing. Random dense matrices that are also used in the random projection [15] and dimensionality reduction, and expander graphs and sparse random graphs that are combinatorial structures [2]. For random sparse graphs, choosing an appropriate sparsity degree "'d"' is also an important issue. So in this section we used a variety of different compressed sensing matrices to compress 256×256 pixel images with sketch size $m = 8000$ [7]. A real-valued Fourier ensemble, an random sparse graphs with sparsity degrees $d = 4$, $d = 8$, $d = 16$, $d = 32$ were selected. Figure 6 shows the recovered images resulting using these sketches, and also their wavelet spectrum. As the figure shows, there is not much difference in the quality of the recovered images. However, there are major differences between using dense and sparse matrices in terms of the required memory resources and also the recovering time. A dense matrix is too large to be stored in memory, and hence secondary storages are essential to store the matrix and accessing to these matrices only can be done one row or one column at a time using function handlers [22]; in contrast, sparse matrices can be stored in main memory very efficiently. Moreover, some expander graphs have explicit construction, but there is no deterministic guarantee for dense matrices. On the other hand, as figure 7 shows, there is major gap between the recovering time for real-valued Fourier sketches and sparse sketch. Although only about ten minutes are enough to recover an image when real-valued Fourier matrices are used, this time is more than 30 minutes for sparse matrices. Even between the sparse matrices the matrix with least sparsity degree has much less recovering time compare to the others. In summary, dense sketches have a major advantage in the fast recovering times, while sparse matrices with sparsity degree $d = 4$ can be stored more efficiently in memory, but their recovery time is longer. There is no need to use sparse matrices with sparsity degree > 4. Finally, there is not much difference in the quality of the recovered images.

V. Enhancing the quality of the recovered image

A. Quality Improvement

1) Bilateral Filtering: A bilateral filter [18], [17] is an edge-preserving filter useful for imaging. Whereas many filters are convolutions in the image domain, a bilateral filter also operates in the image's range . Rather than replacing a pixel's value with simply a weighted average of its neighbors, a pixel's value is replaced by a weighted average of its neighbors in x, y, and intensity. This preserves sharp edges by systematically excluding pixels from the other side of the discontinuity.

[7]other values of m like $m = 5000$ and $m = 20000$ also led to similar results

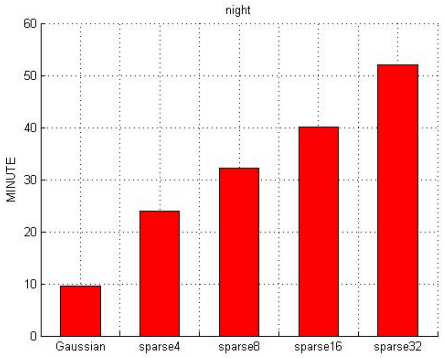

Fig. 7. Recovering time of the figure 6

(a) Manhattan Norm minimization in wavelet domain (min l1)

(b) Total Variance minimization in space domain (min TV)

Fig. 8. Recovering a 256*256 image from a sketch of size m=8000 using l1-minimization and min-TV methods

Although the bilateral filtering will not sharpen an image and it blurs the smooth areas, it increase the marginal confidence in edges.

The basic idea of the bilateral filtering is to apply the filter both in the domain and the range of an image what traditional filters do in its domain. Two pixels can be close to each other, meaning that they occupy nearby spatial location, or they can be similar to each other, meaning that they have nearby values, possibly in a perceptually meaningful fashion. This filter combines domain and range filtering, thereby enforcing both geometric and photometric locality. Combined filtering can be described as follows

$$b(x) = k^{-1} \int_{-\infty}^{\infty} \int_{-\infty}^{\infty} f(\sigma) c(|x - \sigma|) s(|f(x) - f(\sigma)|) d\sigma$$

where k^{-1} is the normalization constant, $c|x - \sigma|$ is a metric for the geometric distance of the pixels [8], and $s(|f(x) - f(\sigma)|)$ is a a metric for the photometric distance of the pixels.

2) Minimize Square Loss Unsharp Mask: In this section we propose a method to reduce the noise and sharpen the image simultaneously. This method is based on the square loss minimization and regression in machine learning [21] and adjusts a set of parameters from the training data, in order to minimize the square loss which we will describe below. This step is very similar to the optimal unsharp mask method [20]

[8]for instance a Gaussian metric $c|x - \sigma| = \alpha e^{\frac{|x-\sigma|^2}{\beta}}$

which is used to sharpen the scanned images and eliminate the noise injected by the scanner.

Before explaining the Bilateral Noise-Reduction Sharpening (BNS) algorithm, we very briefly describe the ordinary unsharp mask method [20]. Suppose F is the original image and G is the blurred and noisy recovered image. The desired estimate for F, using unsharp mask method is obtained by adding a high pass filter to the blurred image to get the edges and then add the result to the blurred images. So it will be:

$$\hat{F}(x,y) = G(x,y) + \lambda(\mathcal{H} \otimes G(x,y)),$$

where $\mathcal{H}$ is the high pass filter convolved with the original image. However, there are two major reasons why the ordinary unsharp mask is not appropriate for the task of sharpening recovered images and noise reduction. First, this method not only does not reduce the noise level, but it also amplifies the noises as the sharpness points. Moreover, this methods sharpens the points uniformly, and hence by choosing λ too low the image edges will not be enhanced as we desire, and by choosing λ too high there might be some over-enhancement in some parts of the image, make the picture appear unnatural.

So we need to use an adaptive version of the unsharp mask method that reduces the noise as a part of the algorithm and besides, the value λ at each point should depend on the sharpness level at that point. Hence, the sharpening process will be of the form:

$$\hat{F}(x,y) = G(x,y) + \lambda_{G(x,y)}(\mathcal{H} \otimes G(x,y)),$$

Of course, the problem will be how to compute $\lambda_{G(x,y)}$. As we will explain below, the value $\lambda_{G(x,y)}$ only depends on the sharpness class at the point (x,y). We will use a supervised square loss minimization training algorithm in order to find optimum values for $\lambda_{G(x,y)}$. We will use different images of different kinds as the training set. Compute the sharpened image from the blurred recovered image and using the Gaussian regression method, we try to minimize the square loss between the sharpened image and the primitive[9] image in order to find the optimal values of $\lambda_{G(x,y)}$. The training process, which is very similar to OUM [20] is as follow:

Laplacian of Gaussian operator (LoG) is a high pass filter that is widely used in the edge detection, it is defined as:

$$LoG(x,y) = -\frac{1}{\pi\sigma^4}\left(1 - \frac{x^2+y^2}{2\sigma^2}\right)e^{-\frac{x^2+y^2}{2\sigma^2}}$$

Now let DLoG be a 9×9 discrete approximation for LoG, then we have:

$$g_{LoG}(x,y) = (DLog \otimes G(x,y))$$

So $g_{LoG}(x,y)$ is a metric for the edge-strength at each pixel. Now in order to be able to learn the parameters based on the edge-strengths we need to classify the pixel based on their edge strength. So we define:

$$C_n(x,y) = \lfloor g_{LoG}(x,y) + 0.5 \rfloor$$

So each pixel is classified to the nearest integer approximating it, however this classification is still very noisy. in order to eliminate the noise which is amplified up we apply a median filter on the edge-strengthen

$$c(x,y) = \mathcal{M} \otimes c_n(x,y)$$

In summary $c(x,y)$ denotes the real (noiseless) class of pixel based on its edge strength. Now for any pixel at position (x,y), $\lambda_{G(x,y)}$ only depends on the class of the edge strength at that point and since the classes of the edge strengths are bounded integer values, the optimal values of $\lambda_{G(x,y)}$ can be learned by using different training images and trying to minimize the square loss between the original and the reconstructed images. So we have the following regression [21]problem:

$$\sum_{i,j} |F(x,y) - G(x,y) - (\lambda_{G(x,y)}(\mathcal{H} \times G(x,y))|^2$$

which is a regression problem and can be solved using Gauss's method and pseudoinverse matrix.

3) Our Bilateral Noise Reduction Sharpening (BNS) Quality Improvement Algorithm: The l1-minimization and min-TV methods discussed above give only approximation for the original image. First of all this approximation is noisy so it is desirable to reduce the noise level of the recovered image. Furthermore, the recovered image is smooth and the sharpness details are removed from it so it may be desirable to find a way to increase the sharpness of the image in order to make it look more natural. The bilateral filter solely is not enough for this task. It cannot sharpen the image, and it may even blur the smooth areas more. Moreover, it cannot reduce the noise level of the image. The square loss unsharp mask solely is not enough either. Since the recovered image is too smooth, the edges in the original image cannot be classified correctly by this method as there is a lack of confidence because of the loss of information in the wavelet domain.

However, by first using the bilateral filtering to increase the confidence at the edges and then applying the adaptive unsharp mask, it is possible to first increase the confidence at edges and then classify the pixels based on their edge-strength. This will reduce the noise level and increase the image sharpness simultaneously. So the proposed algorithm will be as follow:

Algorithm 1 Bilateral Noise Reduction Sharpening (BNS) algorithm

1) Recover the image using the min TV algorithm.
2) Apply the bilateral filtering to the image in order to increase the edge confidence.
3) Computer the edge-strength class at each pixel $c(x,y)$.
4) Find the corresponding $\lambda_{G(x,y)}$[10].
5) Compute the DLoG highpass filter at each pixel: $\mathcal{H} \otimes G(x,y)$.
6) For each pixel at position (x,y) output $\hat{F(x,y)} = G(x,y) + \lambda_{G(x,y)}(\mathcal{H} \otimes G(x,y))$.

[9]unblurred

(a) Row recovered image using the min TV method with $m = 8000$ measurements

(b) The image after only applying the bilateral filtering

(c) The image after performing the BNS algorithm

Fig. 9. Improving the quality of a recovered image using the suggested BNS algorithm

VI. Algorithm Results and conclusion

Figures 9,10 show the results of applying the algorithm on recovered images. Because of space constraint we omit the detailed explanation. The algorithm tries to reduce the noise while sharpening the image. The recovered images of previous section, in combination with original images were used as training data to find optimal parameter λ. Figure 10 is a zoom in of figure 9 to one eye. It may be seen that there is almost no improvement on using solely bilateral filtering but using the proposed algorithm makes the quality of the image slightly better. Although we had relative improvement, the improvement in the quality is not very significant. There is still a lot of space for finding better algorithms with much more remarkable results. Recently new sharpening methods like Deblurring Using Regularized Locally-Adaptive Kernel Regression [23] and adaptive bilateral sharpening [19] has been also proposed. Trying to sharpen the recovered images using Deblurring Using Regularized Locally-Adaptive Kernel Regression is our future work.

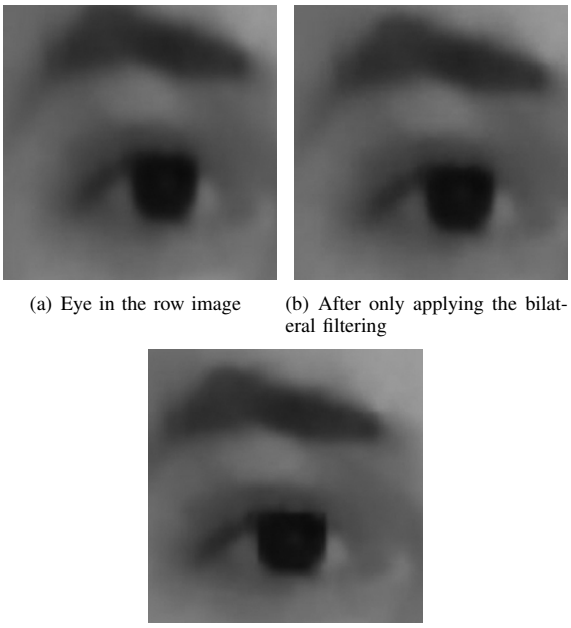

(a) Eye in the row image

(b) After only applying the bilateral filtering

(c) After performing the BNS algorithm

Fig. 10. One eye in the figure 9 zoomed in

Acknowledgment

We would like to thank Adam Finkelstein for his costructive suggestions, and from Radu Berinde [7] for his great helps in implementing the sparse matrices, and Justin Romberg for the great $l1$-magic package [22] which was used in the image recovery process.

References

[1] S. Jafarpour, W. Xu, B. Hassibi, R. Calderbnak *Efficient Compressed Sensing using High-Quality Expander Graphs*, Preprint.

[2] S. Vadhan *Expander Graphs* , Lecture 8, Pseudorandomness course, Harvard University, Fall 2004.

[3] L. Bassalygo, M. Pinsker *Complexity of an optimum nonblocking switching network without reconnections* , Problem in Information Transmission, vol 9 no 1, pp. 289-313, 1973.

[4] L. Applebaum, S. Howard, S. Searle, and R. Calderbank, *Chirp sensing codes: Deterministic compressed sensing measurements for fast recovery.* Preprint, 2008.

[5] V. Tarokh. *Reed-Solomon frames from Vandermonde Matrices*.

[6] F. Parvaresh and B. Hassibi, *List decoding for compressed sensing.* In preparation.

[7] R. Berinde, P. Indyk. *Sparse recovery using sparse random matrices*, http://people.csail.mit.edu/indyk/report.pdf, 2008.

[8] V. Guruswami, C. Umans, S. Vadhan *Unbalanced Expanders and Randomness Extractors from Parvaresh-Vardy Codes.*, proceedings of the 22nd Annual IEEE Conference on Computational Complexity , 2007.

[9] E. Candes, J. Romberg, T. Tao *Exact signal reconstruction from highly incomplete and inaccurate measurements*, IEEE Trans. Information Theory, 2005.

[10] E. Candes, J. Romberg, T. Tao *Robust uncertainty principles: Exact signal reconstruction from highly incomplete frequency information*, IEEE Trans. on Info. Theory, 52(2):489509, 2006.

[11] E. Candes, J. Romberg, T. Tao *Stable signal recovery from incomplete and inaccurate measurements*, Comm. Pure Appl. Math., 59(8):12081223, 2006.

[12] R. Baraniuk. *Compressive Sensing* , Lecture notes in IEEE Signal Processing magazine, 2007.

[13] E. Candes, B. Wakin. *"people hearing without listening:" An introduction to compressive sampling* , California Institute of technology, 2007.

[14] D. Donoho. *compressed sensing* , IEEE Trans.Information Theory 52, no.4, pp. 1289-1306, 2006.

[15] R. Baraniuk, M. Davenport, R. DeVore, M. Wakin. *A simple proof of the Restricted Isometry Property of Random Matrices* , Constr. Approx., 2007.

[16] M. Wakin, J. Laska, M. Duarte, D. Baron, S. Saravorham, D. Takhar, K. Kelly, R. Baraniuk *An architecture for compressive imaging*.

[17] A. Finkelstein, T. Weyrich *Computer Graphics* , Computer Science course notes, http://www.cs.princeton.edu/courses/archive/spring08/cos426/.

[18] C. Tomasi and R. Manduchi *Bilateral Filtering for Gray and Color Images* , Proceedings of the IEEE International Conference on Computer Vision, Bombay, India, 1998.

[19] B.Zhang and J. Allebach *Adaptive Bilateral Filter for Sharpness Enhancement and Noise Removal* , Proceedings of the IEEE International Conference on Image Processing, ICIP, 2007.

[20] S. Kim and J. P. Allebach *Optimal unsharp mask for image sharpening and noise removal* , J Electron Imaging, vol. 14, no. 2, pp. 0230071 02300713, 2005.

[21] T. Hastie, R. Tibshirani and J. Friedman *The Elements of Statistical Learning: Data Mining, Inference, and Prediction*, Springer.

[22] J. Romberg, E. Candes *l1-magic : Recovery of Sparse Signals* , http://www.acm.caltech.edu/l1magic/downloads/l1magic.pdf, Caltech, 2007.

[23] H. Takeda, S. Farsiu, and P. Milanfar, *Deblurring Using Regularized Locally-Adaptive Kernel Regression*, IEEE Trans. on Image Processing, vol. 14, no. 4, pp550-563, April 2008.